nature structural & molecular biology

An asymmetric interface between the regulatory and core particles of the proteasome

Geng Tian[1], Soyeon Park[1], Min Jae Lee[1,2], Bettina Huck[1], Fiona McAllister[1], Christopher P Hill[3], Steven P Gygi[1] & Daniel Finley[1]

The *Saccharomyces cerevisiae* proteasome comprises a 19-subunit regulatory particle and a 28-subunit core particle. To be degraded, substrates must cross the core particle–regulatory particle interface, a site for complex conformational changes and regulatory events. This interface includes two aligned heteromeric rings, one formed by the six ATPase (Rpt) subunits of the regulatory particle and the other by the seven α subunits of the core particle. The Rpt C termini bind to intersubunit cavities in the α-ring, thus directing core particle gating and proteasome assembly. We mapped the Rpt C termini to the α subunit pockets, using a cross-linking approach that revealed an unexpected asymmetry: one side of the ring shows 1:1 contacts of Rpt2-α4, Rpt6-α3 and Rpt3-α2, whereas on the opposite side, the Rpt1, Rpt4 and Rpt5 tails each cross-link to multiple α pockets. Rpt–core particle cross-links are all sensitive to nucleotides, implying that ATP hydrolysis drives dynamic alterations at the core particle–regulatory particle interface.

The proteasome plays a central role in ubiquitin-dependent protein degradation. Its substrates probably number in the hundreds, and given that they are involved in diverse pathways such as those involving cell cycle control, DNA repair, transcription and inflammation, the proteasome functions as an integral component of many cellular regulatory mechanisms. Accordingly, its activity is under intricate control[1–3].

The proteasome core particle (or the 20S proteasome) is a barrel-like complex of four stacked heptameric rings of subunits, with the proteolytic active sites facing the interior space[4]. Substrates gain entry to the core particle's interior through a gated axial channel[5–12]. Disruption of the gate enhances ubiquitin-dependent protein degradation in yeast[13]. The channel is formed by the outermost subunits of the core particle, which constitute the α-rings, whereas the proteolytic sites are found in the central β-rings. The eukaryotic proteasome is thought to have evolved from a simpler complex, which may have resembled the present-day PAN (proteasome-activating nucleotidase) protease complex of archaea[14–17]. The core particle of both the PAN protease complex and the eukaryotic proteasome have an $\alpha_7\beta_7\beta_7\alpha_7$ structure, but in the former, the rings are homomeric, whereas in the latter, they are heteromeric.

The proteasome regulatory particle (also known as the 19S particle and PA700) pairs with the core particle to form the proteasome holoenzyme (the 26S complex). The regulatory particle can be divided into a core particle–proximal ten-subunit base assembly and a distal nine-subunit lid assembly[1,18]. Like the core particle, the regulatory particle contains subunits that are related to the PAN complex. However, PAN is a homohexameric ATPase ring complex, whereas the regulatory particle includes a heterohexameric ATPase ring as a part of the base. In yeast, this 'Rpt ring' is formed by Rpt1–Rpt6. Other regulatory particle components are poorly understood, but several appear to mediate the recognition and disassembly of ubiquitin chains[1]. ATP hydrolysis by the Rpt ring drives unfolding of protein substrates[2,19–21]. In the majority of PAN complexes, only two ATP molecules are bound per ring, with two subunits being bound to ADP and two unoccupied[14]. The Rpt ring is thought to pull substrates into its central pore with sufficient force to promote unfolding of substrate structural domains that are too large to traverse the pore[22,23]. Continued translocation directs the unfolded substrate from the regulatory particle channel into the core particle, where it is degraded.

Recent studies of the archaeal PAN complex and the related actinobacterial protease ARC have provided major structural insights[15,16]. PAN was found to be a trimer of dimers, at least within its core particle–distal oligonucleotide–oligosaccharide binding (OB) and coiled-coil (CC) domains. Accordingly, the eukaryotic Rpt ring assembles through dimeric precursors (Rpt1 and Rpt2, Rpt4 and Rpt5, and Rpt3 and Rpt6)[24–26].

The C-terminal segments, or tails, of the Rpt proteins are conserved in evolution (**Supplementary Fig. 1a**) and critical for proteasome function. They extend from the body of the Rpt ring toward the core particle and insert into pockets formed at α-α subunit interfaces[9]. For some tails, insertion results in opening of the core particle channel[5–8,27]. The tails also regulate regulatory particle assembly in yeast[28,29], and the regulatory particle–core particle interaction[30,31], most likely through insertion of the tails into the α pockets of the core particle[32]. There are six Rpt tails and seven α pockets, a symmetry mismatch indicating

[1]Department of Cell Biology, Harvard Medical School, Boston, Massachusetts, USA. [2]Department of Applied Chemistry, Kyung Hee University, Gyeonggi-do, Republic of Korea. [3]Department of Biochemistry, University of Utah School of Medicine, Salt Lake City, Utah, USA. Correspondence should be addressed to D.F. (daniel_finley@hms.harvard.edu).

Received 25 April; accepted 18 August; published online 30 October 2011; doi:10.1038/nsmb.2147

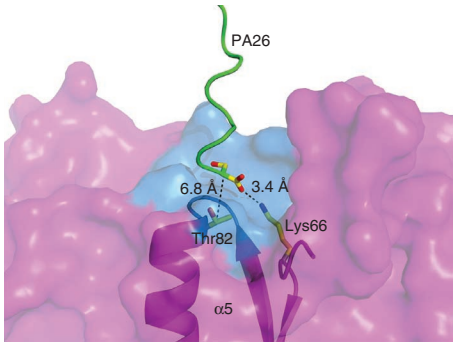

Figure 1 Structural basis for the cross-linking strategy. Detail of a representative α pocket (α4-α5), showing residues used for cross-linking. A surface representation of the α5 subunit is shown along with a cartoon representation of the last 12 residues of a PA26 subunit inserted into the α4-α5 pocket[9]. α5 is in purple, with the pocket surface of this subunit in blue. A partial backbone of the α5 subunit is presented in cartoon mode, with the side chain of Thr82 (the residue substituted with cysteine and used for cross-linking) and Lys66 of the α5 subunit as well as the C-terminal carbonyl group of PA26 presented in stick mode. The distance between the C terminus of PA26 and the pocket lysine Lys66, as well as that between the C terminus and Thr82, are labeled (PDB: 1FNT[11]).

that not all α pockets can be simultaneously occupied in this manner. Despite the critical roles played by the regulatory particle–core particle interface, its organization has remained unknown.

In this study, we used mutagenesis and cysteine-specific cross-linking to probe contacts between the Rpt proteins and the core-particle α subunits. The results define the relative arrangement of the 13 subunits that make up the stacked ring assemblies of the regulatory particle–core particle interface and reveal that this interface is unexpectedly asymmetric. Three neighboring Rpt proteins insert into specific α pockets, whereas, on the opposite side of the Rpt ring, each Rpt tail can be found cross-linked to more than one α pocket. These results suggest the existence of several interconvertible populations of proteasomes, which differ in the positioning of the unoccupied α pocket. Our findings may explain specific characteristics of the structure of the proteasome as observed by electron microscopy[17,33–35]. Nucleotide affects cross-linking efficiency for every α-Rpt pair, suggesting that the engagement between α and Rpt subunits is dynamically regulated by ATP hydrolytic cycles, with the principal stabilizing contacts alternating from subunit to subunit as ATP is bound and hydrolyzed asynchronously.

RESULTS

The regulatory particle–core particle interface

We used chemical cross-linking to investigate the interaction between the Rpt and α subunits. We first substituted cysteine in place of the C-terminal residue of each Rpt protein, which is a critical residue for both the assembly and gating functions of the Rpt tails[8,9,29] (see **Supplementary Fig. 1a** for sequence alignments of Rpt C termini). Its principal feature is thought to be the main chain carboxylate, rather than the side chain[5,6,8,9]. Each carboxylate is proposed to form a salt bridge to the ε-amino group of a specific α subunit lysine residue[9], a residue that, for six of the seven α subunits, aligns with K66 in the α subunit of the PAN complex (the 'pocket lysine'). Accordingly, deletion of the C-terminal residue has substantial phenotypic effects for most Rpts[29]. Substitution mutations, which are expected to preserve the salt bridge to the pocket lysine, were for the most part well tolerated, though under conditions of proteolytic stress, such as high temperature, hypomorphic function could be observed (**Supplementary Fig. 2** and data not shown). Analysis of purified proteasomes from these mutants indicated that the regulatory particle–core particle interaction is, depending on context, either not detectably perturbed or minimally perturbed (**Supplementary Fig. 2**).

The introduction of cysteines into the α-ring was guided by the structure of a complex between PA26 and the yeast core particle[9]. PA26 is a homoheptameric activator of the core particle. Although unrelated to the regulatory particle, PA26 also binds the core particle through C-terminal tail insertion into the α pockets, and has served as a model for regulatory particle–core particle interactions[6,9]. In particular, PA26 C termini form salt bridges with the pocket lysines. Thus, we substituted a residue in the α pocket that is proximal to the C terminus of PA26. This residue is directly adjacent to the beginning of the α2 helix in each α subunit and is surface-exposed on the interior of the pocket (**Fig. 1**; for an alignment of α subunits in this region, see **Supplementary Fig. 1b**). We individually introduced cysteines into each α subunit. These α subunit mutants were then crossed to the *rpt* mutants to create a 6×7 array of double cysteine-substitution mutants. All double-mutant combinations were viable (**Supplementary Fig. 2** and data not shown).

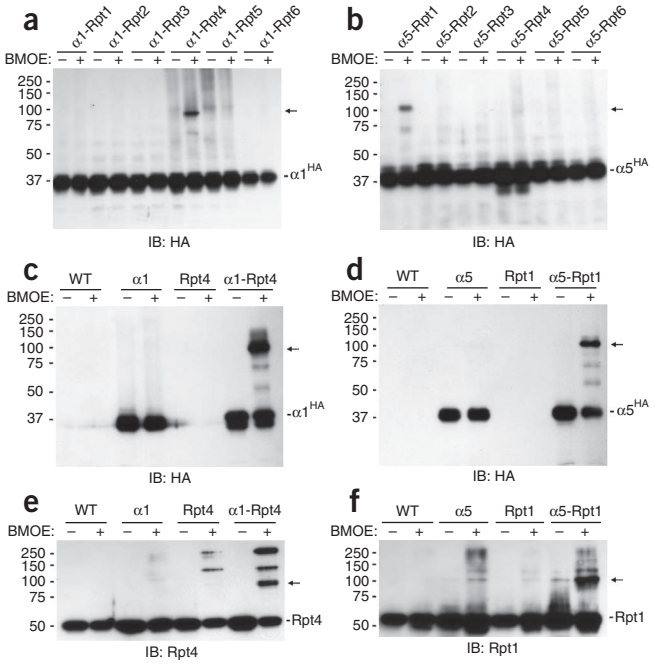

Figure 2 Identification of two α-Rpt subunit pairs by cysteine cross-linking. (**a**,**b**) Whole-cell lysates of yeast were subjected to cross-linking and SDS-PAGE–immunoblot analysis. In each panel, strains contain one α and one Rpt subunit with introduced cysteines. Panels **a** and **b** represent α1-I87C and α5-T82C mutants, respectively. Each panel contains a complete set of Rpt C-terminal mutants, as indicated (Rpt1-N467C, Rpt2-L437C, Rpt3-K428C, Rpt4-L437C, Rpt5-A434C and Rpt6-K405C). A 6×HA tag is present at the C terminus of each α subunit. BMOE (0.1 mM) is a cysteine-cysteine cross-linker; cross-linking proceeded for 1 h at 4 °C. Cross-linked products are marked by an arrow. The antibody used to probe each panel is indicated at bottom. The electrophoretic mobility and molecular mass (in kDa) of protein standards are indicated at left. (**c**–**f**) Purified proteasomes from wild-type yeast or mutant yeasts with either a single cysteine substitution or a double cysteine substitution within the two α-Rpt pairs identified in panels **a** and **b** were subjected to cross-linking and SDS-PAGE–immunoblot (IB) analysis. Panels **c** and **e** for α1–Rpt4; panel **d** and **f** for α5–Rpt1. Here, as below, proteasomes were purified through a protein-A tag appended to Rpn11 (ref. 51).

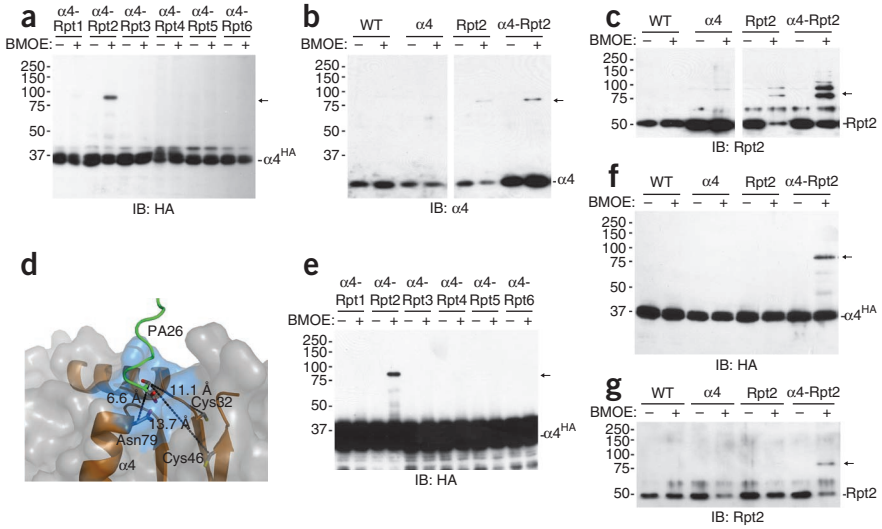

Figure 3 Identification of the α4-Rpt2 pair. (**a**) Whole-cell lysates from α4-N79C RptX double mutants were subjected to cross-linking and SDS-PAGE–immunoblot analysis. See legend to **2a** for details. The cross-linked product is marked by an arrow. The antibody used to probe each panel is indicated at bottom. (**b**,**c**) Cross-linking of α4 to Rpt2 does not strictly require an introduced cysteine in α4. Purified proteasomes from wild-type or mutant yeast with either single or double cysteine substitutions of the Rpt2-α4 pair were cross-linked and subjected to SDS-PAGE–immunoblot analysis. A set of strains in which the α4 subunit was not HA-tagged was used here and the blot was probed with α4-specific antibody. (**d**) Model of the α3-α4 pocket, showing proximity of endogenous cysteine residues (Cys32 and Cys46) to the pocket. The surface of α4 is in gray. Cartoon representation of partial backbone of α4 and the C-terminal tail of PA26 are presented in brown and green, respectively, whereas the pocket surface is highlighted in blue. Cys32 and Cys46, along with Asn79 and C terminus of PA26, are represented in stick mode and the distances between their β-carbons are labeled (PDB: 1FNT[11]). (**e**) Whole-cell lysates from cells expressing HA-tagged wild-type α4 and cysteine-substituted Rpt proteins were subjected to cross-linking, followed by SDS-PAGE–immunoblot analysis. See legend to **a** for details. (**f**,**g**) Purified proteasomes from a set of C32A C46A strains were subjected to cross-linking followed by SDS-PAGE–immunoblot analysis. In lanes marked α4, Asn79 was substituted with cysteine. Those marked Rpt2 are from Rpt2-L437C mutants.

Identification of two α–Rpt subunit pairs

We carried out cross-linking using the divalent cysteine cross-linker bismaleimidoethane (BMOE), whose spacer arm is 8 Å when extended[36,37]. To ensure that BMOE would only generate cross-links to Rpt tails that inserted into a given α pocket, we modeled the space that could be searched by a BMOE molecule anchored at the introduced cysteine residue, using the crystal structure of the yeast core particle[4]. The results indicated that the Rpt tails must gain access to the pocket to achieve cross-link formation.

Our initial scan for cross-linked products in whole-cell lysates allowed mapping of α-Rpt subunit pairings α1-Rpt4 and α5-Rpt1 (**Fig. 2a**,**b**). For example, a cross-link product was found to form in Rpt4-L437C α1-I87C double mutant proteasomes but not in double mutants between α1-I87C and cysteine substitutions of other Rpt proteins (**Fig. 2a**). The cross-link product was visualized through 6× hemagglutinin (HA) epitopes appended to the α subunits at their C termini, which are surface-exposed (**Supplementary Fig. 3**). The apparent molecular mass of the cross-linked products,

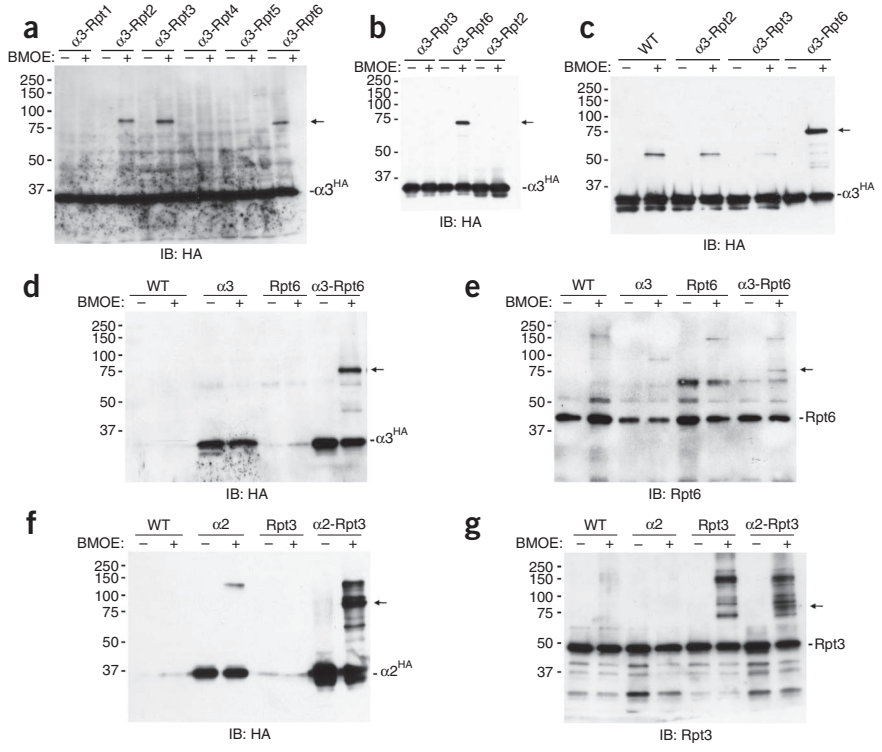

Figure 4 Identification of the α3-Rpt6 and α2-Rpt3 pairs. (**a**) Whole-cell lysates from yeast strains at A_{600} = 5 carrying double cysteine substitutions as indicated were subjected to cross-linking and SDS-PAGE–immunoblot analysis. All strains expressed α3-T81C. For the Rpt mutant set, see legend to **Figure 2a**. Antibody to HA was used to probe for cross-linked products. (**b**) Whole-cell lysates from yeast strains carrying the three identified Rpt-α3 pairs of panel **a** and in exponential growth (A_{600nm} = 1) were subjected to cross-linking and SDS-PAGE–immunoblot analysis. (**c**) Purified proteasomes from wild-type yeast or mutant yeasts with either a single cysteine substitution or a double cysteine substitution within the α3-Rpt6 pair identified in panels **a** and **b** were subjected to cross-linking and SDS-PAGE–immunoblot analysis. (**d**,**e**) Purified proteasomes were subjected to cross-linking and SDS-PAGE–immunoblot analysis. Mutant samples were α3-T81C, Rpt6-K405C and α3-T81C Rpt6-K405C. The blots were probed with antibodies to either HA (to detect α3) or Rpt6. (**f**,**g**) Purified proteasomes were subjected to cross-linking and SDS-PAGE–immunoblot analysis. Mutant proteins were α2-A79C, Rpt3-K428C, and α2-A79C Rpt3-K428C. Blots were probed with antibodies to either HA or Rpt3.

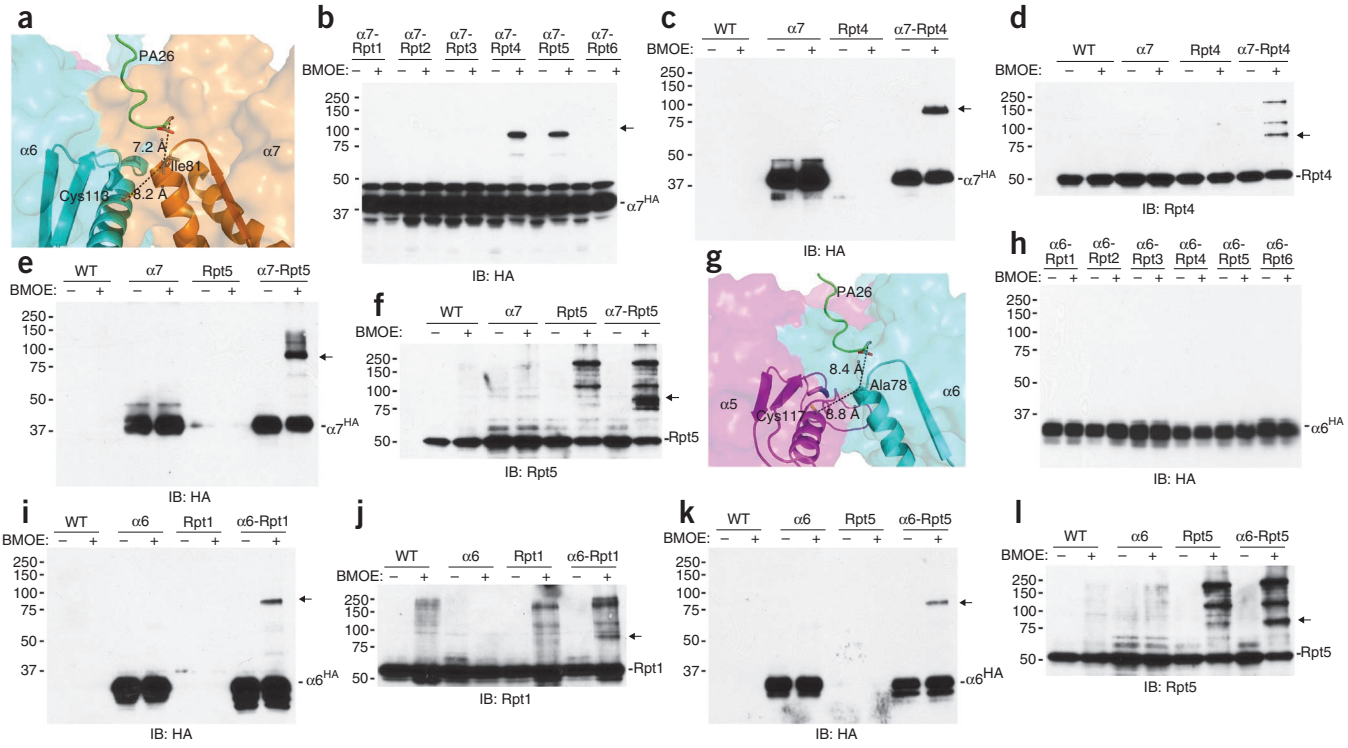

Figure 5 Identification of cross-links for α5-α6 and α6-α7 pockets. (**a**) Model of the α6-α7 pocket showing proximity of endogenous residue Cys113 of α6 to the introduced cysteine (A78C). The two α subunits are in orange and cyan, respectively, and the C terminus of PA26 in green. Partial backbones of the α subunits are in cartoon mode. Side chains of three residues, either a native cysteine or two residues to be substituted with cysteine, are in stick mode, and the distances between their β-carbons are labeled. (**b**) Whole-cell lysates from yeast strains carrying double cysteine substitutions as indicated were subjected to cross-linking and SDS-PAGE–immunoblot analysis. All strains expressed α7-I81C with Cys113 of α6 mutated to alanine. For the Rpt mutants, see legend to **Figure 2a**. (**c**,**d**) Purified proteasomes were subjected to cross-linking and SDS-PAGE–immunoblot analysis. Mutant samples were α7-I81C, Rpt1-N467C and α7-I81C Rpt1-N467C, all of which are purified from strains with Cys113 of α6 substituted with alanine. (**e**,**f**) As in **c** and **d**, except for confirmation of α7-I81C and Rpt5-A434C cross-linking. (**g**) Similar to **a**, model of α5-α6 pocket to show proximity of native cysteine Cys117 in α5 to the position where a cysteine was introduced in α6. The α5 subunit is in magenta, and the others follow the same color scheme as in **a**. (**h**) As in **b**, cross-linking in whole-cell lysates from a set of strains containing the indicated Rpt cysteine substitutions together with the α6-A78C substitution. For Rpt mutants, see legend to **Figure 2a**. (**i**–**l**) Similar as **c**–**f**, except that cross-linking was carried out with α6-A78C and Rpt4-L437A or Rpt5-A434C mutants. All strains in **h**–**l** expressed α5 with Cys117 substituted with alanine.

approximately 80 kD, is consistent with the existence of an adduct between Rpt4 (49 kDa) and α1 (28 kDa) (**Fig. 2a**).

To understand the cross-linking data, it is important to recognize that each α pocket is formed at the interface of two α subunits. Within any αX-αY pocket, where X and Y are any two adjacent α subunits, the penultimate residue of the Rpt is expected to displace the Pro17 turn of αX, which promotes repositioning of the α subunit N termini to form an open gate conformation[5–7], whereas the Rpt C-terminal carboxylate is expected to form a salt bridge with the pocket lysine residue of subunit Y[5,6,9] (**Fig. 1**). The cysteine substitution was placed in subunit αY (α5 in **Fig. 1**), with which the C-terminal three residues of PA26, and presumably the Rpt subunits, form main chain hydrogen bond interactions. Thus, in the case of Rpt1 for example, cross-linking to α5 indicates that Rpt1 might affect the state of the Pro17 turn and N termini of α4. Consequently, we use the names of both subunits when referring to an α pocket. The pockets are α1-α2, α2-α3, α3-α4, α4-α5, α5-α6, α6-α7 and α7-α1.

Our finding that the Rpt4 C terminus inserts into the α7-α1 pocket was unexpected, given the sequence characteristics of this pocket. Because there are six Rpt proteins apposed to seven α subunits, one of the α pockets must be unoccupied at a given time, or at least not occupied by an Rpt C terminus. The α7-α1 pocket was previously hypothesized to be the 'empty' pocket of the α-ring, because it lacks a pocket lysine[9] (**Supplementary Fig. 1b**).

To test whether the α1-Rpt4 and α5-Rpt1 cross-links were generated in mature, fully assembled proteasomes, we repeated the cross-linking with affinity-purified proteasomes (**Fig. 2c**–**f**). Proteasomes were purified from wild-type cells, α1-I87C mutants, Rpt4-L437C mutants and from the corresponding double mutants. The pattern of cross-linking was similar to that seen in whole-cell extracts, and in addition, we observed that cross-linking was strictly dependent on the presence of both α1-I87C and Rpt4-L437C substitutions (**Fig. 2c**). When these reactions were probed with antibodies to Rpt4, the specificity of the cross-link for the mutated form of α1 was also apparent (**Fig. 2e**). Similar experiments confirmed insertion of Rpt1 into the α4-α5 pocket (**Fig. 2d**,**f**).

Identification of an α4-Rpt2 pair

A third cross-link observed in whole-cell lysates was formed between α4 and Rpt2 (**Fig. 3a**). We purified proteasomes from the α4-Rpt2 double mutant and the corresponding single mutants, and we repeated the cross-linking. Although cross-link formation was fully dependent on Rpt2-L437C, it proved to be only partially dependent on the α4-N79C substitution (**Fig. 3b**,**c**). This result suggested that a native cysteine residue in α4 might be capable of cross-linking to Rpt2. We therefore examined the structure of the α3-α4 pocket, modeling its interaction with Rpt tail elements on the PA26–yeast core particle co-crystal structure. As suspected, two native cysteines (Cys32 and Cys46) in α4 were

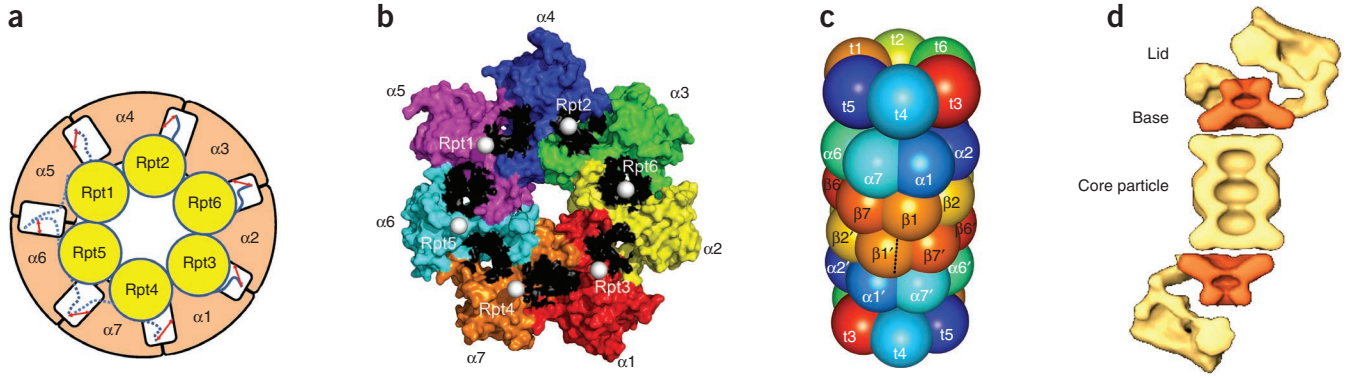

Figure 6 Model of the base–core particle complex. (**a**) Proposed model mapping the six Rpt tails to the seven α pockets of the core particle. The α subunits are in tan with white intersubunit pockets. Rpt subunits are in yellow with blue C-terminal tails. Solid arrows from the C-terminal tail of an Rpt represent unique cross-linking between an Rpt and a specific α pocket. Dashed lines from the C-terminal tail indicate cross-linking of an Rpt to multiple α pockets. (**b**) Proposed model for mapping the six Rpt tails into the seven α pockets of the core particle. The α-ring is represented as a molecular surface with each subunit in a different color. The pockets formed between subunits are colored black. The six Rpt C termini are represented by white spheres, the positions of which are modeled from the C termini of the D2 domain of CDC48 (PDB: 3CF1)[54]. (**c**) Ball model of base–core particle complex. The C2-fold symmetry axis of the core particle lies at the interface between β1 and β1′, as shown. (**d**) Core particle–regulatory particle misalignment of the proteasome holoenzyme as revealed by cryoelectron microscopy. Averaged images of negatively stained *Drosophila melanogaster* proteasomes. The density assigned to the Rpt ring is given in orange, the remainder of the proteasome in tan. Adapted with permission from reference 34.

potentially accessible to the C-terminal tail in its modeled position, with Cys46 being the more surface-exposed of the two (**Fig. 3d**). If some structural flexibility of the Rpt2 tail within the pocket is assumed, Cys46 should not be too distant from the tail to be cross-linked.

To test whether Cys32 or Cys46 might account for the unidentified cross-links, we tested HA-tagged but otherwise wild-type α4 for cross-linking to the standard panel of Rpt cysteine mutants. In whole-cell extracts, we again observed specific cross-linking to Rpt2, supporting the involvement of native cysteine residues in cross-link formation (**Fig. 3e**). Cys32 and Cys46 were therefore jointly substituted with alanine. Under these conditions, α4-Rpt2 cross-linking was fully dependent on the α4-N79C substitution (**Fig. 3f**,**g**). Thus, cysteine residues at multiple positions within the α3-α4 pocket can apparently cross-link to Rpt2.

α3-Rpt6 and α2-Rpt3 pairs

The data above, together with the known subunit arrangement of the Rpt ring[38] (**Supplementary Fig. 4**), constrain the possible assignments of the remaining three α-Rpt pairs. For example, because α3 abuts α4 and Rpt6 abuts Rpt2, the α4-Rpt2 pair should be flanked by an α3-Rpt6 pair; that is, the Rpt6 tail is expected to insert into the α2-α3 pocket. However, when cross-linking was carried out in whole-cell extracts from cells in the post-diauxic shift phase, we reproducibly observed α3 to contact both Rpt2 and Rpt3, in addition to Rpt6 (**Fig. 4a**). By contrast, whole-cell extracts from exponential phase cells yielded only the expected α3-Rpt6 cross-link (**Fig. 4b**). Purified proteasomes from post-diauxic-shift–phase cells showed cross-linking only between α3 and Rpt6, and these cross-links required both α3-T81C and Rpt6-K405C substitutions (**Fig. 4c**–**e**). In summary, our data indicate that the α2-α3 pocket is the receptor for the Rpt6 tail, and they also provide an initial indication that under some physiological conditions, Rpt–α pocket mispairing or ambiguity might occur. The mispaired Rpt C termini, Rpt2 and Rpt3, flank Rpt6 on either side. One possibility is that ambiguous alignment of the Rpt6 tail is characteristic of certain proteasome assembly intermediates.

Assignment of the α3-Rpt6 pair implies that an α2-Rpt3 pair should be formed in the next position, working clockwise around the ring. In cross-linking studies with crude extracts, we could not visualize this putative species (**Supplementary Fig. 5a**). However, in purified proteasomes, the predicted cross-linked species, the formation of which requires the α2-A79C substitution (**Fig. 4f**), could be observed at the correct size (arrow). These data support assignment of Rpt3 as a ligand of the α1-α2 pocket. However, the Rpt3-K428C substitution

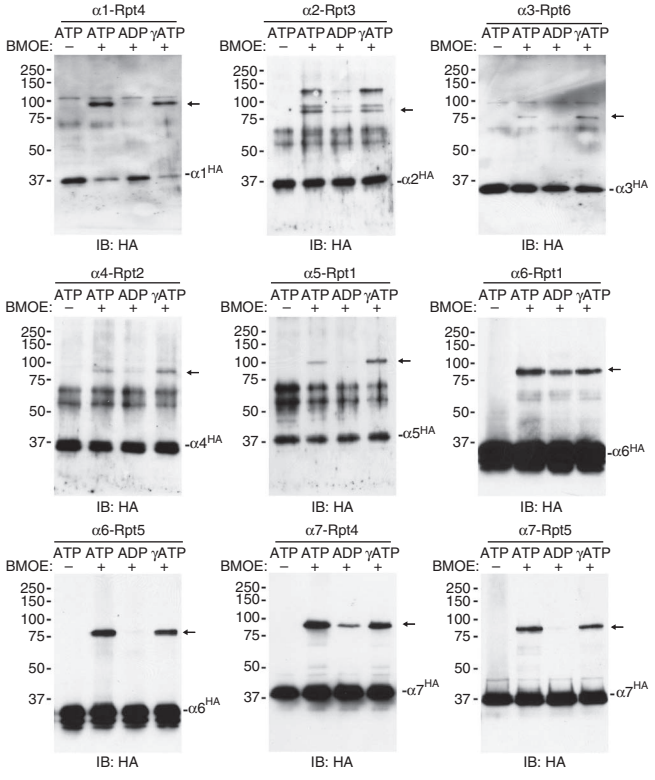

Figure 7 Effect of nucleotides on cross-linking between α and Rpt subunits. Each panel shows the result of cross-linking purified proteasomes from a different double mutant, as indicated, with each double mutant showing cross-linking being represented. Immunoblots of these samples were probed with antibody to HA.

led to some cross-linking in the absence of α2-A79C, resulting in unidentified background bands that may have reduced the intensity of the signal for the α2-Rpt3 pair (**Fig. 4g**).

The α5-α6 and α6-α7 pockets

The two remaining unassigned α pockets, α5-α6 and α6-α7 (**Fig. 5**), showed background cross-link formation to endogenous cysteines (**Supplementary Fig. 5b**,**c**). The responsible cysteine residues were identified and mutated to alanine (**Fig. 5a**,**g**). In this genetic background, we observed specific cross-linking of the α6-α7 pocket to both Rpt4 and Rpt5, in extracts and with purified proteasomes (**Fig. 5b**–**f**). The α5-α6 pocket did not form detectable cross-links in extracts but cross-linked specifically to Rpt1 and Rpt5 in purified proteasomes (**Fig. 5h**–**l**).

The results above indicate that several Rpt proteins can cross-link to multiple α pockets. Rpt5, for example, is capable of cross-linking to both α5-α6 and α6-α7 pockets (**Fig. 5**). Moreover, Rpt4 cross-links not only to α6-α7 (**Fig. 5b**–**d**) but also, as described above, to α7–α1 (**Fig. 2**). Finally, Rpt1 cross-links to both α5-α6 (**Fig. 5i**,**j**) and, as shown in **Figure 2**, α4-α5. Thus, the register of tail-pocket insertion is apparently not strictly fixed over four neighboring α pockets, in marked contrast to the remaining three pockets (α1-α2, α2-α3 and α3-α4). Additionally, we found no evidence for a defined unoccupied α pocket, the existence of which has generally been assumed, based on the excess number of α pockets over Rpt tails. Our working model of the regulatory particle–core particle interface is shown in **Figure 6**.

The regulatory particle–core particle interface is dynamic

ATP hydrolysis by the proteasome is essential for its ability to degrade proteins and provides the driving force for translocation of the substrate protein through the regulatory particle–core particle interface. Based on studies of related ATP-dependent proteases, nucleotide hydrolysis presumably drives substrate translocation, at least in part, by guiding movement of the pore-1 loop within the axial substrate translocation channel[21,39,40]. However, far from the pore-1 loop, ATP hydrolysis may also be expected to direct movement of the C-domains, from which the Rpt tails emerge[40,41]. We therefore tested whether the engagement of Rpt tails within their cognate α pockets is regulated by ATP.

We purified proteasomes in the presence of 0.1 mM ATP and subjected them to cross-linking after the addition of ADP, ATP or ATPγS to 1 mM. We found that all of the α-Rpt contacts behaved similarly, in that cross-linking was enhanced by ATP in comparison to ADP (**Fig. 7**). A trivial explanation for the suppression of cross-linking by ADP would be that ADP drives dissociation of the core particle and regulatory particle. Previous work has shown that for yeast proteasomes, this is not the case[42], and we confirmed under our conditions that little or no dissociation of the core particle and regulatory particle occurs (**Supplementary Fig. 6**).

ATPγS, a nonhydrolyzable ATP analog, stimulated α-Rpt cross-linking, in comparison to ATP, for some cross-linking pairs but not for others (**Fig. 7**). These effects were modest in comparison to those seen when comparing ATP to ADP. The α2-α3 α3-α4 and α4-α5 pockets, all showing enhanced cross-link formation with ATPγS, form a continuous block of subunits on one side of the Rpt ring—notably, the side characterized by fixed Rpt-α cross-links. Pockets on the opposite face of the ring showed either no stimulation or a slight suppression in the presence of ATPγS. Consistent with these trends, Rpt1 cross-linking to α4-α5 was stimulated by ATPγS but cross-linking to α5-α6 was not. These data suggest that α-Rpt cross-link formation may serve as a sensitive probe to differentiate subtly different functional states of the mature proteasome holoenzyme.

DISCUSSION

The dynamic nature of the regulatory particle–core particle interface was first apparent when the substrate translocation channel of the core particle was identified and found to assume open and closed states in a regulated manner[11,12]. The organization of this extensive interface has remained unknown, despite fragmentary data from many studies, based on either the two-hybrid method, cross-linking or other approaches[27,30,33,43–48]. In general, these studies can be only partially reconciled with each other and with our current understanding of the topologies of the Rpt and α-rings. In contrast to all previous work, we have used mutagenesis to focus exclusively on the contacts between Rpt tails and the α pockets in intact proteasomes. Thus, we have mapped those contacts that are thought to provide the crucial connections between the regulatory particle and the core particle. The final map is complete, self-consistent and compatible with constraints that derive from the known subunit orders of the two rings.

The regulatory particle–core particle contact points show several unanticipated features. Most notably, there is a general asymmetry in the mapping, such that on one side of the Rpt ring, we observe fixed contacts, whereas on the other side of the ring, the C terminus of an Rpt shows flexible contacts, with the capacity to insert into more than one α pocket. The possibility that the flexibility of cross-link formation is in general a peculiarity of BMOE-induced cross-linking was excluded by using other cross-linking methods, including $CuCl_2$-mediated cross-linking[32], in which no linker arm is present (data not shown). As a consequence of the flexibility of Rpt insertion, we did not identify any unoccupied α pocket, although the existence of such a pocket was anticipated based on the Rpt-α subunit symmetry mismatch. Our data suggest a model in which a proteasome sample is composed of distinct subpopulations, each with a different unoccupied pocket. Such subpopulations are likely to interconvert. Thus, an unoccupied pocket, though not fixed or identifiable by cross-linking, may underlie the flexibility in register of Rpt1, Rpt5 and Rpt4. Moreover, the symmetry mismatch between the Rpt and α-rings also dictates that the Rpt tail and the α pockets cannot be aligned in such a way that each tail is proximal to a unique pocket (**Fig. 6b**) because the interpocket angle in the α-ring is 51° and the tail-tail angle is on average 60°. This problem could be minimized if only two tails were engaged at a given time[14] (that is, those tails associated with the ATP-bound subunit), but with the engagement of four tails, some tails would be required to straddle two α pockets.

Notably, the asymmetrical character of the regulatory particle–core particle interface is consistent with existing genetic data, in that strong phenotypes tend to cluster toward the fixed half of the ring. Among Rpt tail mutants, the strongest phenotype is that of Rpt6, which is fixed to the α2-α3 pocket, whereas the weakest phenotype belongs to Rpt1, which shows flexibility in its pocket insertion (ref. 29 and S.P., unpublished data). Similarly, among the α subunits, the α3 mutants show a far more pronounced phenotype than α7 (refs. 12,13). All of the fixed tails—Rpt2, Rpt6 and Rpt3—show strong phenotypes, whether in proteasome assembly or gating[8,29].

The asymmetric character of the regulatory particle–core particle interface described here may help to explain the misalignment in the axes of the Rpt and α-rings observed in electron microscopic analyses of the proteasome. **Figure 6d** provides one example[17,33–35]. Most likely, the regulatory-particle axis fluctuates substantially with respect to the core particle[49], the misaligned orientation described by Bohn *et al.*[33] being an average of many species. Based on our mapping, the asymmetry arising from this misalignment is well correlated with the asymmetry of cross-linking; it was concluded that the axis of the Rpt ring is displaced in the direction of the α2-α3 pocket[33], which is in

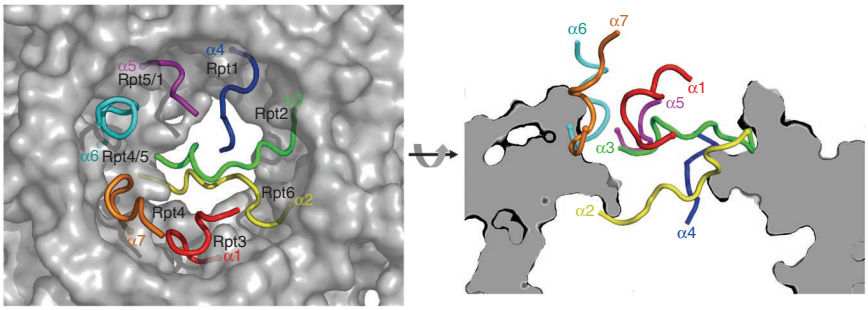

Figure 8 The α subunit N-terminal tails and the Rpt proteins proposed to direct their movements. The left panel is as viewed from the regulatory particle–core particle interface. The closed form of the core particle channel is shown[4]. The N-terminal tails (residues 10–18 of α1, 1–11 of α2, 2–12 of α3, 3–10 of α4, 9–14 of α5, 2–12 of α6 and 4–13 of α7) are shown in cartoon mode and in different colors. The remaining residues are in surface representation, colored in gray. The α-carbon of the last residue (toward the tail's C terminus) of each N-terminal tail is represented as a sphere. The panel at right is a side view of the α-ring gate with the same color scheme as at left. Note that Rpt4 and Rpt6 are positioned to disrupt the N-terminal tails of α7 and α2 but do not open the gate[29], consistent with their lack of an HbYX motif[8] and the minor role in gating played by the peripheral α7 N terminus[12].

the center of the region characterized by fixed cross-links. Indeed, it is possible that the asymmetry of the core particle–regulatory particle interface described in the present study may also underlie the tilted and misaligned regulatory particle–core particle orientation in the PAN holoenzyme[17], despite the homomeric nature of PAN and its corresponding α-ring.

Although our findings define important parameters, especially regarding the fixed contact points, further aspects of the regulatory particle–core particle interaction require more study. Do Rpt tails that insert into two α pockets have a preferred pocket? Does the choice of pocket influence the functional consequences of tail engagement, such as in the assembly, gating and stability of the proteasome? Does the shift of a tail from one pocket to another occur primarily as a consequence of ATP hydrolysis? Is it true that any one of four distinct pockets can be unoccupied in a given proteasome (α4-α5, α5-α6, α6-α7 and α7-α1) or, for example, if α6-α7 is not occupied by Rpt4, is it always occupied by Rpt5?

The cross-linking approach requires the use of α pocket and Rpt tail mutants, which could affect the specificity of insertion. However, the only phenotypes we found were mild. Another caveat to the cross-linking approach is that it monitors the entry of Rpt tails into the α pocket, but not every instance of tail entry is necessarily a functional engagement. An important goal for future work is to determine the functional significance of asymmetry at the interface and whether this a property of the Rpt tails or some other element of the interface. It will be interesting to find mutants in which the symmetry of the interface is altered.

Proposed role of Rpt–core particle contacts in Rpt ring assembly

Mapping of the Rpt–core particle contacts also provides new information on assembly of the Rpt ring. Previous studies have suggested that Rpt ring assembly in yeast is guided, in part, by pre-existing α-rings[28,29,32,50]. Of particular importance to this model is that both α subunit mutants and Rpt mutants show the accumulation of Rpt ring assembly intermediates. The Rpt mutants were single amino acid deletions at the C termini of Rpt4 and Rpt6, the latter showing a stronger phenotype. To date, only the core particle subunit α3 has been implicated in Rpt ring assembly[32]. This subunit might thus be predicted to directly contact one of the Rpts that promote assembly, and indeed, the tail of Rpt6 cross-links specifically to α3. This observation provides further support for the idea that the core particle promotes Rpt ring assembly in yeast and provides a foundation for more precise studies of this complex assembly pathway.

The asymmetry of the regulatory particle–core particle interface may also underlie distinct functional differences among the regulatory particle chaperones, which bind near the C termini of four of the Rpt proteins[24,28,29] to assist in assembly of the Rpt ring. Rpn14 and Nas6, which lie on the fixed side of the ring, can be distinguished genetically from Hsm3 and Nas2, which lie on the flexible side of the ring[24,26,38]. For Rpn14 and Nas6, prior studies suggest that the chaperone-Rpt interaction is competitive with regulatory particle–core particle binding[28,29]. The suggested mechanism involves steric hindrance: insertion of the C-terminal tails of the Rpt proteins may be disfavored by the presence of the chaperones, owing to the proximity of the chaperones to the core particle when they are bound to Rpt proteins[28,29]. A still unidentified release mechanism may obtain for Hsm3 and Nas2 (refs. 25,38,50 and S.P., unpublished data). Thus, insertion of Rpt tails into α pockets of the core particle on the flexible side of the ring may be poorly suited to displace the chaperones.

Rpt C termini and α subunit N termini may co-evolve

Our data raise the possibility that the C-terminal tails of the Rpt subunits have co-evolved with the N-terminal tails of the α subunits, though they are not in contact with one another. For example, Rpt2 has strong gate-opening ability, whereas Rpt4 has not been seen to promote gate opening[8,10,29]. This may be attributed to the HbYX motif of Rpt2 and the absence of such a motif in Rpt4 (ref. 8), but this distinction between Rpt2 and Rpt4 may also result from the nature of the N-terminal tails of the α subunits whose movements they direct. Our cross-linking data indicate that the C-terminal tail of Rpt2, in docking at the α3-α4 pocket, would displace the α3 N-terminal tail from its central position in the closed form of the core-particle gate (**Fig. 8**). On the other hand, engagement of the Rpt4 C-terminal tail would potentially lead to displacement of the N-terminal tail of α7. However, deletion of the α7 tail does not open the core-particle gate, whereas that of α3 does[12]. This difference is consistent with the positioning of these tails within the gate, with the tail of α3 being the most centrally located of any α subunit tail and the tail of α7 tail being peripheral (**Fig. 8**). Rpt4 might also influence the α1 N terminus, which is similarly peripheral (**Fig. 8**). More generally, it is notable that the N termini of the α subunits that show flexible cross-linking all point outwards from the core particle in the closed state of the complex, whereas those showing fixed cross-link formation all follow an inward or lateral path (see **Fig. 8b**).

Coupling of gating to nucleotide hydrolysis

The proteasome undergoes cycles of ATP hydrolysis in both the presence and absence of substrate. Thus, the sensitivity of Rpt–α pocket cross-linking to nucleotide suggests that the tail-pocket interaction is dynamic, a conclusion that appears to apply to each Rpt protein. The low cross-linking efficiencies seen in the presence of ADP do not necessarily indicate complete dissociation of the Rpt tail from α pockets or a complete lack of involvement of ADP-bound Rpt

proteins in gating. Indeed, ADP is effective in stabilizing regulatory particle–core particle association, at least for yeast proteasomes[42,51], although whether this effect is related to the engagement of Rpt tails with the core particle is not known. The nucleotide-free form of the ATPase might show the most radical changes in orientation of the C-domain, but we cannot yet probe that state because wild-type proteasomes dissociate under such conditions.

Based on our finding that Rpt tails engage less strongly with the core particle in the presence of ADP rather than ATP or ATPγS, we postulate that, as ATP is hydrolyzed by successive subunits in the Rpt ring, the contacts between the regulatory particle and core particle undergo a cycle of motions in response. Structural studies of related hexameric ATPases suggest that the nucleotide is hydrolyzed in a rotary mechanism[52,53], in which one of the highly populated species contains two ATP molecules and two ADP molecules, with two ATPase subunits not interacting with a nucleotide. We favor an analogous model for the proteasome[14]. Our finding that ATP and ADP have distinct effects on the strength of interaction between the Rpt C termini and the α pockets therefore suggests that strong engagement of only a subset of tails, possibility as few as two, is needed to open the core particle gate. The Rpt tails that strongly activate the gate—Rpt2, Rpt3 and Rpt5—alternate around the ring. Consequently, the gate would remain open through cycles of ATP hydrolysis that proceed around the ring, even if ADP and unbound Rpt subunits adopt conformations that do not promote engagement of their C termini.

METHODS

Methods and any associated references are available in the online version of the paper at http://www.nature.com/nsmb/.

Note: Supplementary information is available on the Nature Structural & Molecular Biology website.

ACKNOWLEDGMENTS

We thank W. Tansey (Vanderbilt University Medical Center) and C. Mann (Commissariat à l'énergie atomique et aux énergies alternatives (CEA)/Saclay) for antibodies, B.-H. Lee for helpful discussions, A. Matouschek for comments on the manuscript and W. Baumeister for permission to reproduce **Figure 6D**. Funding was provided by US National Institutes of Health grants to D.F. (R37GM43601), C.P.H. (R01 GM59135) and S.G. (GM67945). S.P. was supported by a fellowship from the Charles A. King Trust and M.J.L. by the American Health Assistance Foundation.

AUTHOR CONTRIBUTIONS

G.T., S.P., C.P.H. and D.F. contributed to the conception of this project. G.T., S.P. and B.H. contributed to strain construction and genetic analysis. G.T, S.P. and M.J.L. conducted cross-linking studies. F.M. and S.P.G. carried out mass spectrometry on cross-linked samples. G.T., C.P.H. and D.F. were largely responsible for the manuscript.

COMPETING FINANCIAL INTERESTS

The authors declare no competing financial interests.

Published online at http://www.nature.com/nsmb/.
Reprints and permissions information is available online at http://www.nature.com/reprints/index.html.

1. Finley, D. Recognition and processing of ubiquitin-protein conjugates by the proteasome. *Annu. Rev. Biochem.* **78**, 477–513 (2009).
2. Schrader, E.K., Harstad, K.G. & Matouschek, A. Targeting proteins for degradation. *Nat. Chem. Biol.* **5**, 815–822 (2009).
3. Demartino, G.N. & Gillette, T.G. Proteasomes: machines for all reasons. *Cell* **129**, 659–662 (2007).
4. Groll, M. *et al.* Structure of 20S proteasome from yeast at 2.4 A resolution. *Nature* **386**, 463–471 (1997).
5. Yu, Y. *et al.* Interactions of PAN's C-termini with archaeal 20S proteasome and implications for the eukaryotic proteasome-ATPase interactions. *EMBO J.* **29**, 692–702 (2010).
6. Stadtmueller, B.M. *et al.* Structural models for interactions between the 20S proteasome and its PAN/19S activators. *J. Biol. Chem.* **285**, 13–17 (2010).
7. Rabl, J. *et al.* Mechanism of gate opening in the 20S proteasome by the proteasomal ATPases. *Mol. Cell* **30**, 360–368 (2008).
8. Smith, D.M. *et al.* Docking of the proteasomal ATPases' carboxyl termini in the 20S proteasome's alpha ring opens the gate for substrate entry. *Mol. Cell* **27**, 731–744 (2007).
9. Förster, A., Masters, E.I., Whitby, F.G., Robinson, H. & Hill, C.P. The 1.9 A structure of a proteasome-11S activator complex and implications for proteasome-PAN/PA700 interactions. *Mol. Cell* **18**, 589–599 (2005).
10. Köhler, A. *et al.* The axial channel of the proteasome core particle is gated by the Rpt2 ATPase and controls both substrate entry and product release. *Mol. Cell* **7**, 1143–1152 (2001).
11. Whitby, F.G. *et al.* Structural basis for the activation of 20S proteasomes by 11S regulators. *Nature* **408**, 115–120 (2000).
12. Groll, M. *et al.* A gated channel into the proteasome core particle. *Nat. Struct. Biol.* **7**, 1062–1067 (2000).
13. Bajorek, M., Finley, D. & Glickman, M.H. Proteasome disassembly and downregulation is correlated with viability during stationary phase. *Curr. Biol.* **13**, 1140–1144 (2003).
14. Smith, D.M., Fraga, H., Reis, C., Kafri, G. & Goldberg, A.L. ATP binds to proteasomal ATPases in pairs with distinct functional effects, implying an ordered reaction cycle. *Cell* **144**, 526–538 (2011).
15. Zhang, F. *et al.* Structural insights into the regulatory particle of the proteasome from Methanocaldococcus jannaschii. *Mol. Cell* **34**, 473–484 (2009).
16. Djuranovic, S. *et al.* Structure and activity of the N-terminal substrate recognition domains in proteasomal ATPases. *Mol. Cell* **34**, 580–590 (2009).
17. Smith, D.M. *et al.* ATP binding to PAN or the 26S ATPases causes association with the 20S proteasome, gate opening, and translocation of unfolded proteins. *Mol. Cell* **20**, 687–698 (2005).
18. Glickman, M.H. *et al.* A subcomplex of the proteasome regulatory particle required for ubiquitin-conjugate degradation and related to the COP9-signalosome and eIF3. *Cell* **94**, 615–623 (1998).
19. Weber-Ban, E.U., Reid, B.G., Miranker, A.D. & Horwich, A.L. Global unfolding of a substrate protein by the Hsp100 chaperone ClpA. *Nature* **401**, 90–93 (1999).
20. Sauer, R.T. & Baker, T.A. AAA+ proteases: ATP-fueled machines of protein destruction. *Annu. Rev. Biochem.* **80**, 587–612 (2011).
21. Glynn, S.E., Martin, A., Nager, A.R., Baker, T.A. & Sauer, R.T. Structures of asymmetric ClpX hexamers reveal nucleotide-dependent motions in a AAA+ protein-unfolding machine. *Cell* **139**, 744–756 (2009).
22. Aubin-Tam, M.E., Olivares, A.O., Sauer, R.T., Baker, T.A. & Lang, M.J. Single-molecule protein unfolding and translocation by an ATP-fueled proteolytic machine. *Cell* **145**, 257–267 (2011).
23. Maillard, R.A. *et al.* ClpX(P) generates mechanical force to unfold and translocate its protein substrates. *Cell* **145**, 459–469 (2011).
24. Saeki, Y., Toh, E.A., Kudo, T., Kawamura, H. & Tanaka, K. Multiple proteasome-interacting proteins assist the assembly of the yeast 19S regulatory particle. *Cell* **137**, 900–913 (2009).
25. Kaneko, T. *et al.* Assembly pathway of the mammalian proteasome base subcomplex is mediated by multiple specific chaperones. *Cell* **137**, 914–925 (2009).
26. Funakoshi, M., Tomko, R.J. Jr., Kobayashi, H. & Hochstrasser, M. Multiple assembly chaperones govern biogenesis of the proteasome regulatory particle base. *Cell* **137**, 887–899 (2009).
27. Gillette, T.G., Kumar, B., Thompson, D., Slaughter, C.A. & DeMartino, G.N. Differential roles of the COOH termini of AAA subunits of PA700 (19S regulator) in asymmetric assembly and activation of the 26S proteasome. *J. Biol. Chem.* **283**, 31813–31822 (2008).
28. Roelofs, J. *et al.* Chaperone-mediated pathway of proteasome regulatory particle assembly. *Nature* **459**, 861–865 (2009).
29. Park, S. *et al.* Hexameric assembly of the proteasomal ATPases is templated through their C termini. *Nature* **459**, 866–870 (2009).
30. Kumar, B., Kim, Y.C. & DeMartino, G.N. The C terminus of Rpt3, an ATPase subunit of PA700 (19 S) regulatory complex, is essential for 26 S proteasome assembly but not for activation. *J. Biol. Chem.* **285**, 39523–39535 (2010).
31. Thompson, D., Hakala, K. & DeMartino, G.N. Subcomplexes of PA700, the 19 S regulator of the 26 S proteasome, reveal relative roles of AAA subunits in 26 S proteasome assembly and activation and ATPase activity. *J. Biol. Chem.* **284**, 24891–24903 (2009).
32. Kusmierczyk, A.R., Kunjappu, M.J., Funakoshi, M. & Hochstrasser, M. A multimeric assembly factor controls the formation of alternative 20S proteasomes. *Nat. Struct. Mol. Biol.* **15**, 237–244 (2008).
33. Bohn, S. *et al.* Structure of the 26S proteasome from *Schizosaccharomyces pombe* at subnanometer resolution. *Proc. Natl. Acad. Sci. USA* **107**, 20992–20997 (2010).
34. Nickell, S. *et al.* Insights into the molecular architecture of the 26S proteasome. *Proc. Natl. Acad. Sci. USA* **106**, 11943–11947 (2009).
35. da Fonseca, P.C. & Morris, E.P. Structure of the human 26S proteasome: subunit radial displacements open the gate into the proteolytic core. *J. Biol. Chem.* **283**, 23305–23314 (2008).
36. Andréasson, C., Fiaux, J., Rampelt, H., Druffel-Augustin, S. & Bukau, B. Insights into the structural dynamics of the Hsp110-Hsp70 interaction reveal the mechanism for nucleotide exchange activity. *Proc. Natl. Acad. Sci. USA* **105**, 16519–16524 (2008).
37. Chen, L.L., Rosa, J.J. Turner, S. & Pepinsky, R.B. Production of multimeric forms of CD4 through a sugar-based cross-linking strategy. *J. Biol. Chem.* **266**, 18237–18243 (1991).

38. Tomko, R.J. Jr., Funakoshi, M., Schneider, K., Wang, J. & Hochstrasser, M. Heterohexameric ring arrangement of the eukaryotic proteasomal ATPases: implications for proteasome structure and assembly. *Mol. Cell* **38**, 393–403 (2010).
39. Martin, A., Baker, T.A. & Sauer, R.T. Pore loops of the AAA+ ClpX machine grip substrates to drive translocation and unfolding. *Nat. Struct. Mol. Biol.* **15**, 1147–1151 (2008).
40. Wang, J. *et al.* Crystal structures of the HslVU peptidase-ATPase complex reveal an ATP-dependent proteolysis mechanism. *Structure* **9**, 177–184 (2001).
41. Bochtler, M. *et al.* The structures of HslU and the ATP-dependent protease HslU-HslV. *Nature* **403**, 800–805 (2000).
42. Kleijnen, M.F. *et al.* Stability of the proteasome can be regulated allosterically through engagement of its proteolytic active sites. *Nat. Struct. Mol. Biol.* **14**, 1180–1188 (2007).
43. Chen, C. *et al.* Subunit-subunit interactions in the human 26S proteasome. *Proteomics* **8**, 508–520 (2008).
44. Satoh, K., Sasajima, H., Nyoumura, K.I., Yokosawa, H. & Sawada, H. Assembly of the 26S proteasome is regulated by phosphorylation of the p45/Rpt6 ATPase subunit. *Biochemistry* **40**, 314–319 (2001).
45. Hartmann-Petersen, R., Tanaka, K. & Hendil, K.B. Quaternary structure of the ATPase complex of human 26S proteasomes determined by chemical cross-linking. *Arch. Biochem. Biophys.* **386**, 89–94 (2001).
46. Davy, A. *et al.* A protein-protein interaction map of the *Caenorhabditis elegans* 26S proteasome. *EMBO Rep.* **2**, 821–828 (2001).
47. Zhang, Z. *et al.* Structural and functional characterization of interaction between hepatitis B virus X protein and the proteasome complex. *J. Biol. Chem.* **275**, 15157–15165 (2000).
48. Gerlinger, U.M., Guckel, R., Hoffmann, M., Wolf, D.H. & Hilt, W. Yeast cycloheximide-resistant crl mutants are proteasome mutants defective in protein degradation. *Mol. Biol. Cell* **8**, 2487–2499 (1997).
49. Walz, J. *et al.* 26S proteasome structure revealed by three-dimensional electron microscopy. *J. Struct. Biol.* **121**, 19–29 (1998).
50. Park, S., Tian, G., Roelofs, J. & Finley, D. Assembly manual for the proteasome regulatory particle: the first draft. *Biochem. Soc. Trans.* **38**, 6–13 (2010).
51. Leggett, D.S. *et al.* Multiple associated proteins regulate proteasome structure and function. *Mol. Cell* **10**, 495–507 (2002).
52. Enemark, E.J. & Joshua-Tor, L. Mechanism of DNA translocation in a replicative hexameric helicase. *Nature* **442**, 270–275 (2006).
53. Thomsen, N.D. & Berger, J.M. Running in reverse: the structural basis for translocation polarity in hexameric helicases. *Cell* **139**, 523–534 (2009).
54. Davies, J.M., Brunger, A.T. & Weis, W.I. Improved structures of full-length p97, an AAA ATPase: implications for mechanisms of nucleotide-dependent conformational change. *Structure* **16**, 715–726 (2008).

ONLINE METHODS

Yeast strains and media. Procedures for the genetic manipulation of yeast, including transformation and tetrad analysis, were carried out as described[55]. Yeast strains are listed in **Supplementary Tables 1** and **2**. All strains used in this study are congenic with strain DF5 (*MAT**a**/MATα lys2-801/lys2-801 leu2-3, 2-112/leu2-3, 2-112 ura3-52/ura3-52 his3-Δ200/his3-Δ200 trp1-1/trp1-1*)[56]. Transformation cassettes[57] were used for protein tagging. Standard synthetic defined media, consisting of 0.7% (w/v) Difco Yeast Nitrogen Base supplemented with amino acids, adenine, uracil and 2% (w/v) dextrose, were used for growth of cells at 30 °C unless specified otherwise. Spotting assays were done as described[58].

Antibodies. The anti-HA antibody was from AbCam (12CA5). Anti-Rpt4 and anti-α4 were from W. Tansey. Anti-Rpt1 and anti-Rpt6 were from C. Mann. Anti-Rpt2, Rpt3, and Rpt5 were from Biomol (PW8260, PW8250 and PW8245, respectively).

Preparation of total cell lysates and cross-linking in total cell lysates. Yeast cells were collected from 5-ml overnight cultures in YPD media and resuspended in 0.5 ml PBS buffer (137 mM NaCl, 2.7 mM KCl, 10 mM Na_2HPO_4, 1.76 mM KH_2PO_4, pH 7.4) supplemented with 5 mM $MgCl_2$ and 1 mM ATP. A 75-µl quantity of glass beads (0.5 mm soda lime, BioSpec) was added to the solution, and the cells were disrupted by sonication (cycles of 15 s of sonication followed by 15 s on ice over 3 min; S-450 digital sonifier, Branson). In one experiment (**Fig. 4b**), lysis was carried out in liquid nitrogen as described[29]. The samples were then centrifuged ($1.6 \times 10^4 g$ for 5 min at 4 °C), and the supernatant was collected and clarified. The protein concentration was estimated with the Coomassie Plus (Bradford) Protein Assay kit (Thermo Scientific) following the manufacturer's instructions, and adjusted to 1 mg ml^{-1}. Cross-linking was achieved by adding 0.1 mM BMOE (Thermo Scientific), followed by incubation on ice for 1 hour[36]. Cross-linking was quenched by addition of 1 mM DTT. The strains used for screening whole-cell lysates by cross-linking are listed in **Supplementary Table 2**.

Purification and chemical cross-linking of proteasomes. All strains used for proteasome purification have a TEV–protein A tag appended to the C terminus of Rpn11 (ref. 51). Proteasome purifications were carried out using IgG-Sepharose (MP Biochemical), with TEV protease (Invitrogen) used for elution (25 mM Tris-HCl, pH7.5, 5 mM $MgCl_2$, 1 mM ATP; details are as described[59], except that $MgCl_2$ was used in all buffers that contained ATP). The cross-linking procedure for purified proteasomes was similar to that for total cell lysates, except that the protein concentration was 0.1 mg ml^{-1}. For cross-linking, purified proteasomes (in concentrated stocks in TEV elution buffer) were diluted into PBS supplemented with 5 mM $MgCl_2$ and 1 mM ATP.

Native PAGE of total cell lysate. Total cell lysates were prepared as described above, and 30 µg of total protein were resolved by 3.5% (w/v) native PAGE, followed by LLVY-AMC overlay assay[60].

Nucleotide-dependence of cross-linking. Proteasomes were purified as described above, except that the IgG-column elution buffer contained 0.1 mM ATP instead of 1 mM ATP. Proteasomes were preincubated with 1 mM ADP, 1 mM ATP or 1 mM ATPγS at 25 °C for 30 min before proceeding with the same cross-linking protocol as given above, at 4°C.

55. Rose, M.D., Winston, F.M. & Heiter, P. *Methods in Yeast Genetics: A Laboratory Course Manual* (Cold Spring Harbor Laboratory Press, Cold Spring Harbor, NY, 1990).
56. Finley, D., Ozkaynak, E. & Varshavsky, A. The yeast polyubiquitin gene is essential for resistance to high temperatures, starvation, and other stresses. *Cell* **48**, 1035–1046 (1987).
57. Janke, C. *et al.* A versatile toolbox for PCR-based tagging of yeast genes: new fluorescent proteins, more markers and promoter substitution cassettes. *Yeast* **21**, 947–962 (2004).
58. Schmidt, M. *et al.* The HEAT repeat protein Blm10 regulates the yeast proteasome by capping the core particle. *Nat. Struct. Mol. Biol.* **12**, 294–303 (2005).
59. Leggett, D.S., Glickman, M.H. & Finley, D. Purification of proteasomes, proteasome subcomplexes, and proteasome-associated proteins from budding yeast. *Methods Mol. Biol.* **301**, 57–70 (2005).
60. Elsasser, S., Schmidt, M. & Finley, D. Characterization of the proteasome using native gel electrophoresis. *Methods Enzymol.* **398**, 353–363 (2005).

doi:10.1038/nsmb.2147

Supplementary materials

An asymmetric interface between the regulatory particle and core particle of the proteasome

Geng Tian, Soyeon Park, Min Jae Lee, Bettina Huck, Fiona McAllister, Christopher P. Hill, Steven P. Gygi, and Daniel Finley

*corresponding author: daniel_finley@hms.harvard.edu

Nature Structural & Molecular Biology doi:10.1038/nsmb.2147

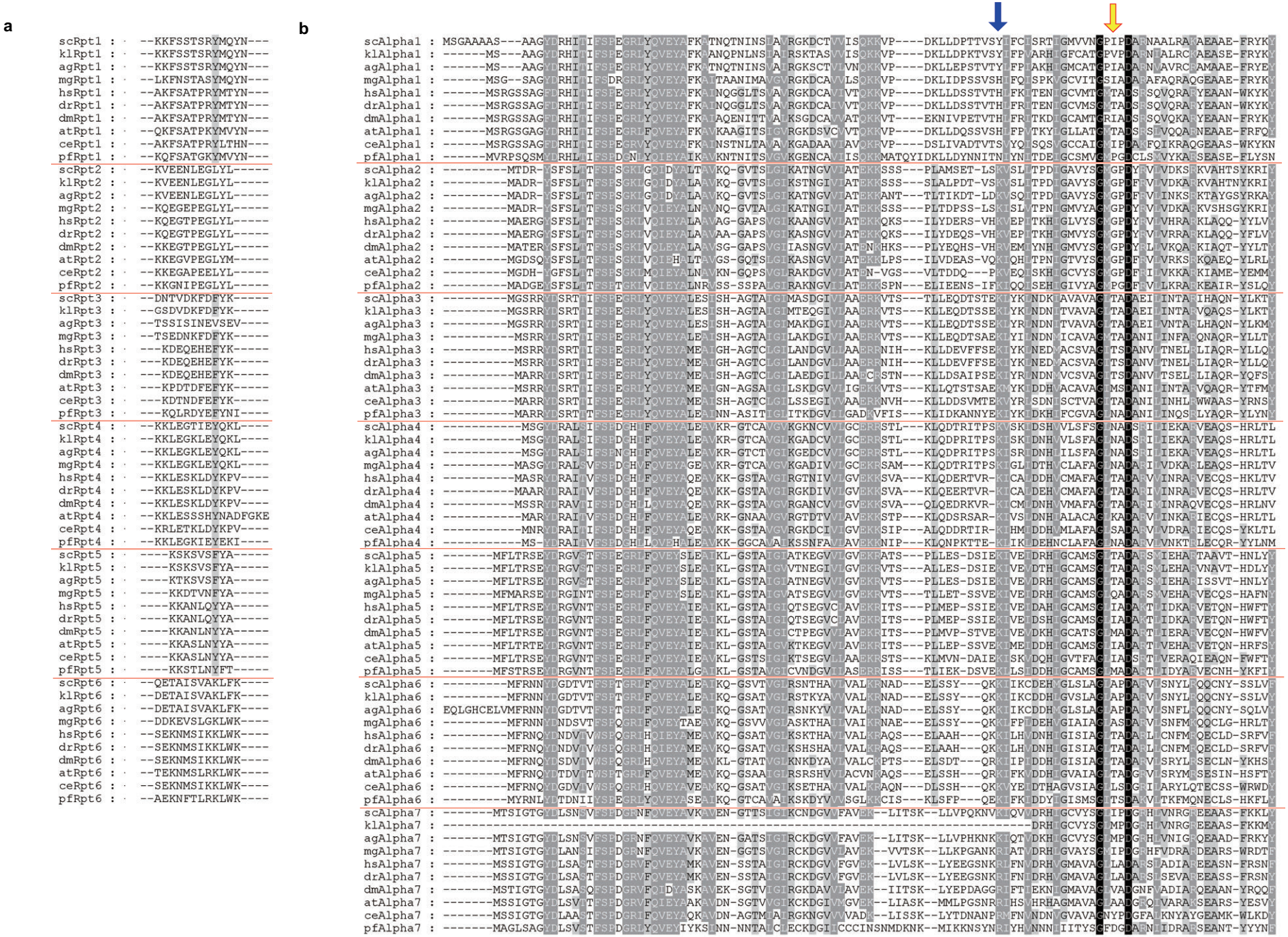

Supplementary figure 1. Sequence alignment of the C-terminal tails of Rpt1–6 (a) and the N-terminal regions of α1–α7 (b) from various species. Black, grey and light-grey shading indicate 100%, 80% and 60% conservation respectively, over the entire α or Rpt family. The conserved residue corresponding to K66 in the T. acidophilum proteasome CP is highlighted by a blue arrow and the non-conserved residue mutated to cysteine within each α pocket is highlighted by a yellow arrow. Abbreviations are: ag: *Ashbya gossypii*; at: *Arabidopsis thaliana*; ce: *Caenorhabditis elegans*; dm: *Drosophila melanogaster*; dr: *Danio rerio*; hs: *Homo sapiens*; kl: *Kluyveromyces lactis*; mg: *Magnaporthe grisea*; pf: *Plasmodium falciparum*; sc: *Saccharomyces cerevisiae*.

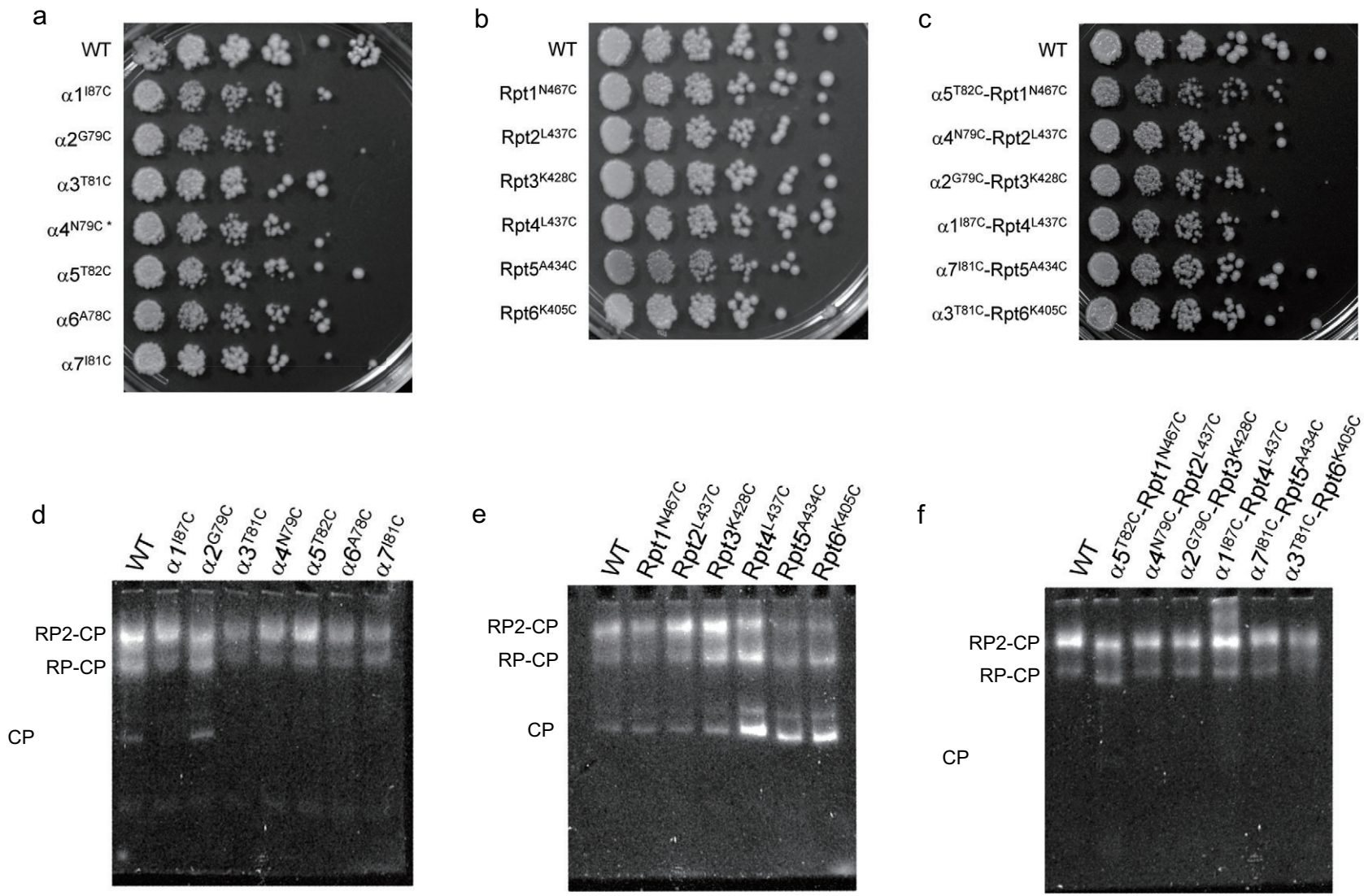

Supplementary figure 2. Evaluation of the effects of introduced cysteines on growth rate and on structural stability of the proteasome. Growth assays of wild type and mutant strains bearing introduced cysteines in α subunits (**a**), Rpt proteins (**b**), and six identified Rpt–α pairs (**c**). Spot assays of cell growth were carried out with 0.05 OD_{600} of cells grown in YPD, resuspended in 250 µl of H_2O, and serially diluted in five-fold increments. The cells were then spotted on YPD plates followed by incubation at 30°C for 48 hr. Note that the RPN11–TevProA allele was not present in these strains. The α4N79C mutant used in all these studies is produced from a strain expressing α4C32A C46A (TG644), which shows the same growth phenotype as wild type under various conditions (Fig. S2 and data not shown). (**d–f**) Total cell lysates of the same set of strains were analyzed by native PAGE followed by overlay assay with LLVY–AMC. Early stationary phase cells were lysed by grinding under liquid N_2. 50 µg of protein were loaded for each strain. Several of the strains are mildly hypomorphic, which is most readily indicated by the enhanced levels of CP in extracts of Rpt4-Rpt6 (ref. 1).

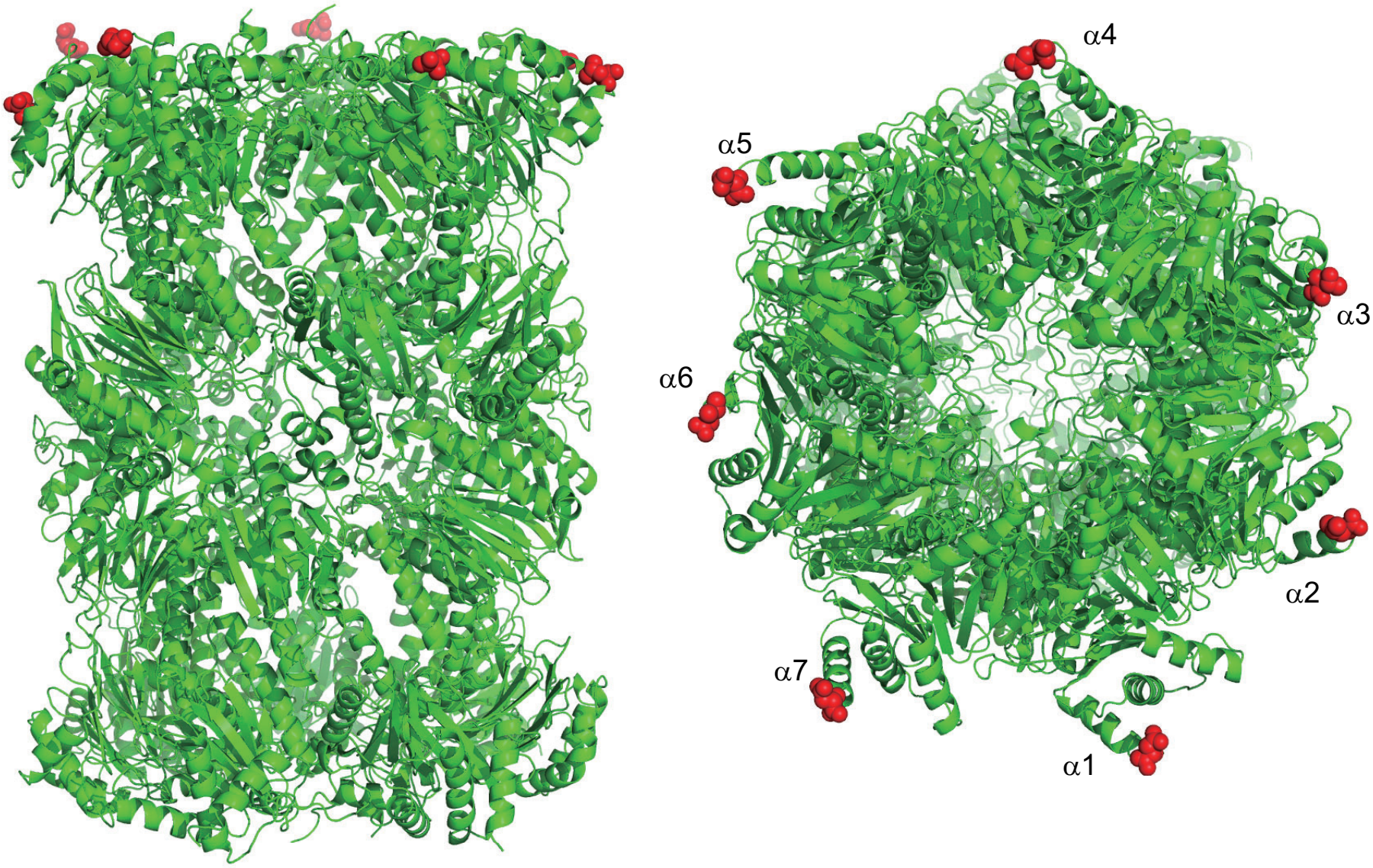

Supplementary figure 3. Surface exposure of α subunit C-termini. The 20S proteasome is shown in cartoon representation painted in green while the C-termini of α subunits are highlighted as red spheres. The exposed position of the C-termini is important because the 6×HA epitope was added to each α subunit at this position; tagging in this way is presumably relatively nonperturbing of α subunit structure. Note that only the C-termini of α1, α2, and α6 are visualized in this 20S proteasome model (PDB: 1RYP[2]); the C-terminal tails of the other α subunits are presumably disordered.

Nature Structural & Molecular Biology doi:10.1038/nsmb.2147

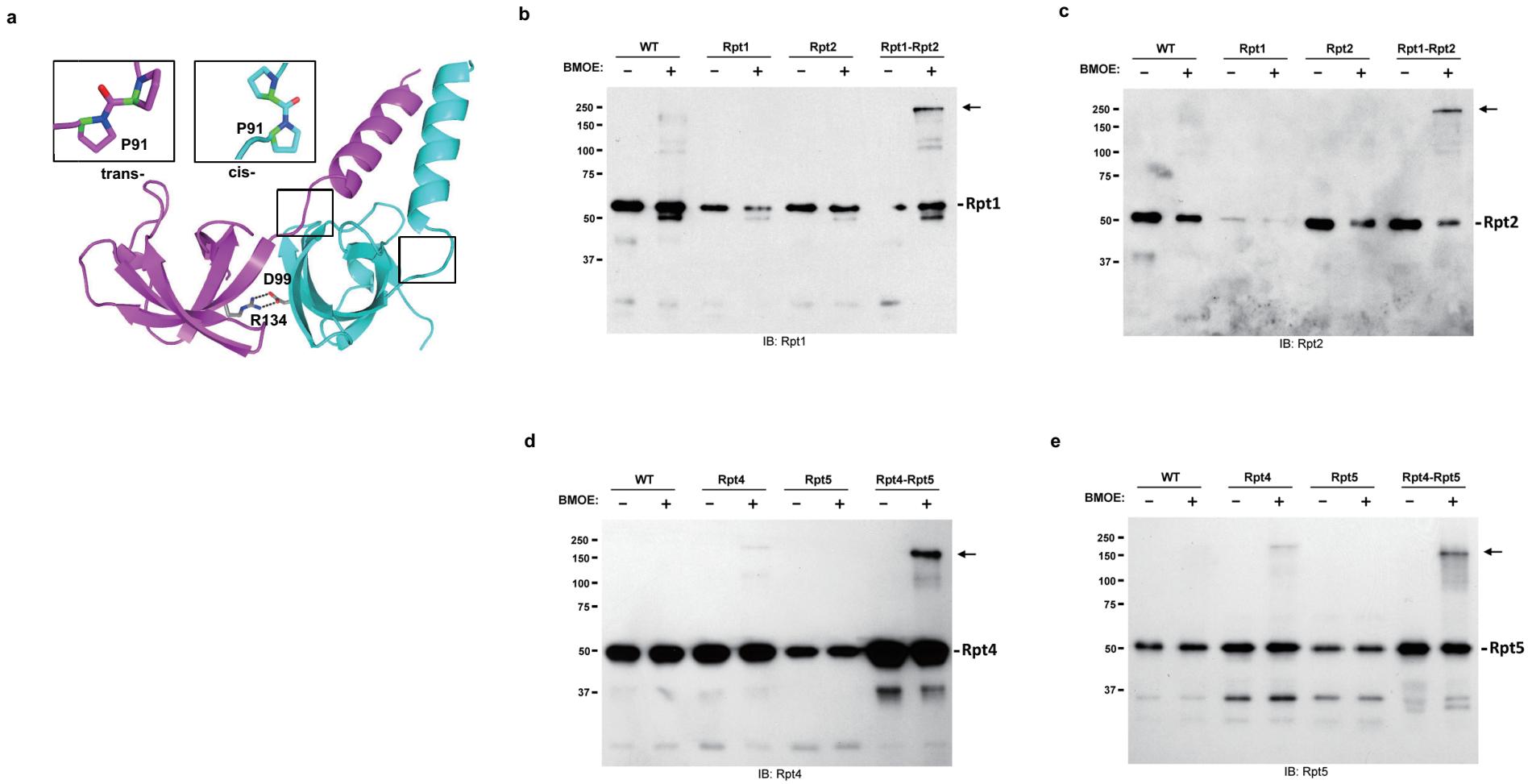

Supplementary figure 4. Pairing between t- and c-type Rpts. In each PAN dimer, one subunit exhibits a cis configuration of the main chain at proline 91, while its partner contains a trans-proline residue. The former is known as a c-type subunit and the latter t-type. The intra-dimer interface of PAN is also characterized by two residues within neighboring OB domains (Asp99 from the c-type subunit and Arg134 from the t-type) that form a salt-bridge[3],[4]. The eukaryotic Rpt ring assembles via dimeric precursors, each composed of one c-type and one t-type subunit[5]-[7]. This figure shows that the Rpt proteins of yeast proteasomes are specifically paired as Rpt1–Rpt2, Rpt4–Rpt5, and (by default) Rpt3–Rpt6. This conclusion is in agreement with Tomko et al[3]. Residues for crosslinking are those implicated in formation of the intradimer salt bridge[4]. (a) Cartoon representation of a dimeric pair of t-type PAN subunit and c- type subunit. t-type PAN is represented in magenta and c-type PAN in cyan. Insets show the configuration of P91 in each type of subunit. The intradimer salt bridge is highlighted in sticks mode. (**b–c**) Identification of the Rpt1-Rpt2 pair. Crosslinking experiments were performed on base subcomplexes from wild type yeast or mutant yeasts, and analyzed by SDS-PAGE and immunoblotting. Mutant proteins were Rpt1-R173C, Rpt2-E111C, and the double, Rpt1-R173C Rpt2-E111C. The two blots are loaded with the same samples but probed with antibodies to either Rpt1 or Rpt2, as indicated. Crosslinked products are marked by arrows. (**d–e**) Identification of the Rpt4-Rpt5 pair. Mutant proteins were Rpt4-R145C, Rpt5-E84C, and Rpt4-R145C Rpt5-E84C. Methods as in panel **b–c** except that whole proteasomes were used for crosslinking.

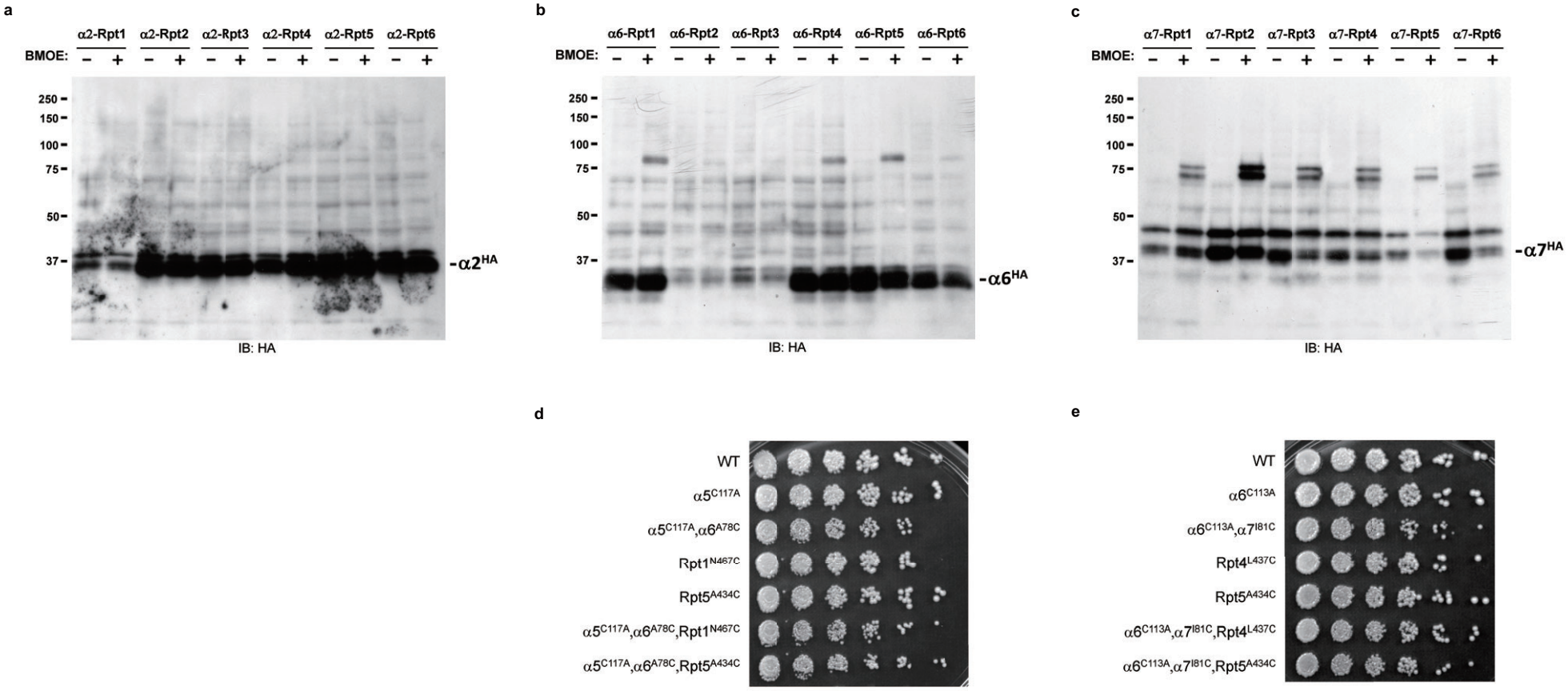

Supplementary figure 5. Whole cell lysate screening for crosslinking partners of α2, α6, and α7 subunits. With whole cell lysates, no crosslinked product was detected for α2 (panel **a**) paired with any of the Rpts. Results for α6 (panel **b**) and α7 (panel **c**) were inconclusive due to a nonspecific crosslinked product with a size similar to that of the specific Rpt-α pair observable using purified proteasomes (Fig. 5). Several lanes are underloaded (lanes 1 and 2 of Fig. S5a, lanes 3–6 of Fig. S5b). As shown in Fig. 5a and 5g of the main text, these nonspecific crosslinked products are formed with cysteines from neighboring α subunits, i.e., C117 of α5 and C113 of α6, respectively. Mutating these cysteines to alanines gives rise to little or no growth phenotype, as shown in panels **e** and **f**.

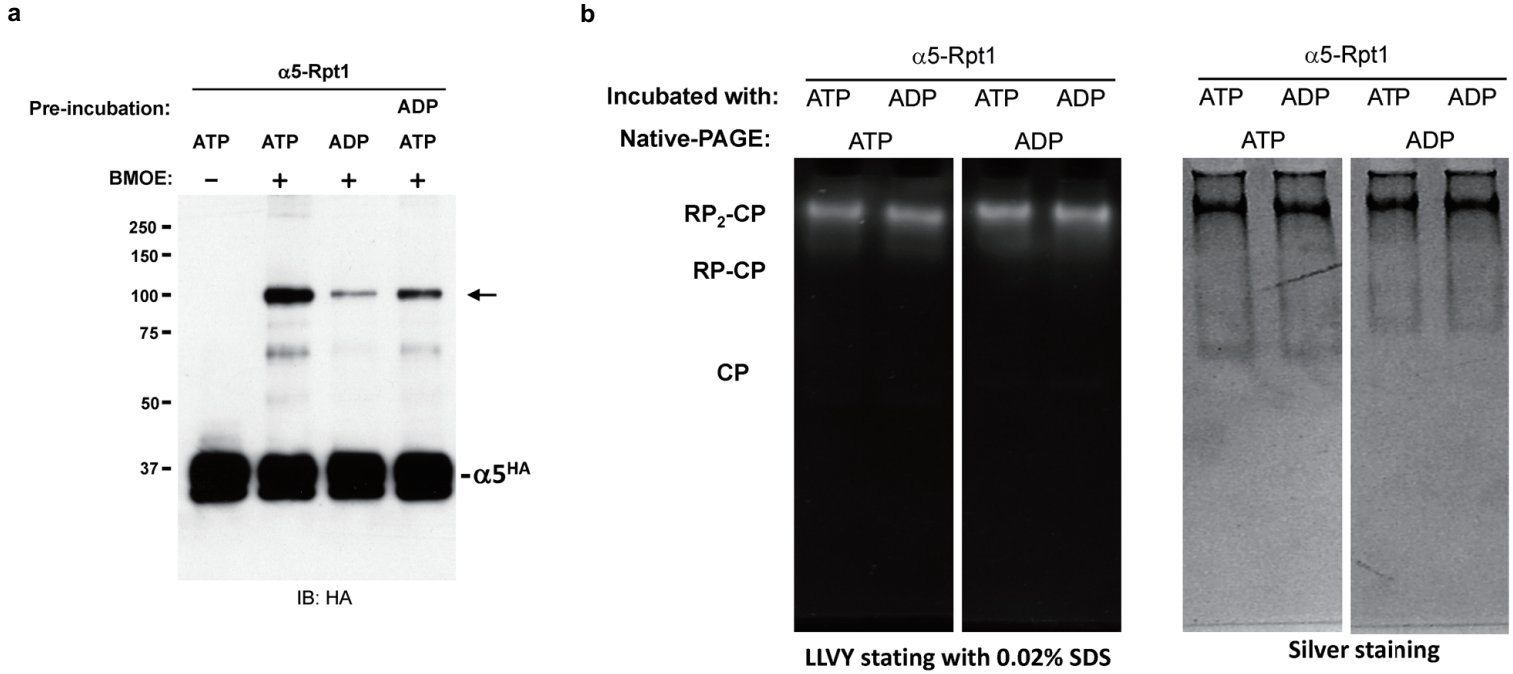

Supplementary figure 6. RP-CP association is not significantly affected by the presence of different nucleotides. (**a**) α5-T82C Rpt1-N467C proteasomes were subjected to crosslinking after 30 min incubation with 1 mM ATP, 1 mM ADP, or 1mM ATP following a 30 min pre-incubation with 1 mM ADP. Crosslinking was assayed by SDS-PAGE followed by immunoblotting. (**b**) Incubation with either ATP or ADP does not affect the distribution of proteasome species (RP_2–CP, RP–CP and CP) for either wild type or mutant (α5-T82C Rpt1-N467C) proteasomes.

Supplementary table 1. Yeast strains used in this study

Strain		Figure
	Part A: Strains used for purification of proteasomes and crosslinking*	
sDL66	MAT*a*	2,3,4,5,S4
TG430	MAT*a scl1::scl1-I87C-6HA (HYG)*	2
TG431	MAT*a pre8::pre8-G79C-6HA (HYG)*	4
TG432	MAT*a pre9::pre9-T81C-6HA (HYG)*	4
SP106	MAT*a pre6::pre6-N79C (URA)*	3
TG434	MAT*a pup2::pup2-T82C-6HA (HYG)*	2
TG989	MAT*a pre5::pre5-A78C-6HA (HYG) pup2::pup2-C117A (TRP)*	5
TG807	MAT*a pre10::pre10-I82C-6HA (HYG) pre5::pre5-C113A (TRP)*	5
TG603	MATα *rpt1::rpt1-N467C (KAN)*	2
TG992	MATα *rpt1::rpt1-N467C (KAN) pup2::pup2-C117A (TRP)*	5
SP79	MATα *rpt2::rpt2-L437C (KAN)*	3
SP56	MATα *rpt3::rpt3-K428C (KAN)*	4
TG607	MATα *rpt4::rpt4-L437C (NAT)*	2
TG772	MATα *rpt4::rpt4-L437C (NAT) pre5::pre5-C113A (TRP)*	5
TG1000	MATα *rpt5::rpt5-A434C (NAT) pup2::pup2-C117A (TRP)*	5
TG1139	MATa *rpt5::rpt5-A434C (NAT) pre5::pre5-C113A (TRP)*	5
TG611	MATα *rpt6::rpt6-K405C (NAT)*	4
TG446	MATα *rpt1::rpt1-N467C (KAN) pup2::pup2-T82C-6HA (HYG)*	2,7,S6
TG1004	MATα *rpt1::rpt1-N467C (KAN) pup2::pup2-T82C-6HA (HYG) pup2::pup2-C117A (TRP)*	5,7
SP212	MATα *rpt2::rpt2-L437C (KAN) pre6::pre6-N79C (URA)*	3
TG468	MATα *rpt3::rpt3-K428C (KAN) pre8::pre8-G79C-6HA (HYG)*	4,7
TG480	MATα *rpt4::rpt4-L437C (NAT) scl1::scl1-I87C-6HA (HYG)*	2,7
TG795	MATa *rpt4::rpt4-L437C (NAT) scl1::scl1-I87C-6HA (HYG) pre5::pre5-C113A (TRP)*	5,7
TG1012	MATα *rpt5::rpt5-A434C (NAT) pre10::pre10-I82C-6HA (HYG) pup2::pup2-C117A (TRP)*	5,7
TG1141	MATα *rpt5::rpt5-A434C (NAT) pre10::pre10-I82C-6HA (HYG) pre5::pre5-C113A (TRP)*	5,7
TG512	MATα *rpt6::rpt6-K405C (NAT) pre9::pre9-T81C-6HA (HYG)*	4,7
TG456	MATα *rpt2::rpt2-L437C (KAN) pre9::pre9-T81C-6HA (HYG)*	4
TG470	MATα *rpt3::rpt3-K428C (KAN) pre9::pre9-T81C-6HA (HYG)*	4
TG651	MATα *pre6::pre6-C32A,C46A-6HA (HYG)*	3
TG653	MATα *pre6::pre6-C32A,C46A,A79C-6HA (HYG)*	3
TG669	MATα *rpt2::rpt2-L437C (KAN) pre6::pre6-C32A,C46A-6HA (HYG)*	3
TG693	MATα *rpt2::rpt2-L437C (KAN) pre6::pre6-C32A,C46A,N79C-6HA (HYG)*	3,7

TG199	MATα *rpt1::rpt1-R173C(TRP1)*	S4
TG203	MATα *rpt2::rpt2-E111C(HYG)*	S4
TG211	MATα *rpt4::rpt4-R145C(NAT)*	S4
TG215	MATα *rpt5::rpt5-E84C(KAN)*	S4
TG223	MATα *rpt1::rpt1-R173C(TRP1) rpt2::rpt2-E111C(HYG)*	S4
TG247	MATα *rpt4::rpt4-R145C(NAT) rpt5::rpt5-E84C(KAN)*	S4
Part B: Strains used for spotting assay and native PAGE of total cell lysate**		
Sub61	MATα	S2,S4
TG577	MAT*a scl1::scl1-I87C-6HA (HYG)*	S2
TG579	MAT*a pre8::pre8-G79C-6HA (HYG)*	S2
TG581	MAT*a pre9::pre9-T81C-6HA (HYG)*	S2
TG646	MAT*a pre6::pre6-C32A C46A N79C-6HA (HYG)*	S2
TG585	MAT*a pup2::pup2-T82C-6HA (HYG)*	S2
TG587	MAT*a pre5::pre5-A78C-6HA (HYG)*	S2
TG589	MAT*a pre10::pre10-I82C-6HA (HYG)*	S2
SP47	MATα *rpt1::rpt1-N467C (KAN)*	S2
TG641	MATα *rpt2::rpt2-L437C (KAN)*	S2
TG643	MATα *rpt3::rpt3-K428C (KAN)*	S2
SP304	MATα *rpt4::rpt4-L437C (NAT)*	S2
SP309	MATα *rpt5::rpt5-A434C (NAT)*	S2
SP311	MATα *rpt6::rpt6-K405C (NAT)*	S2
TG530	MATα *rpt1::rpt1-N467C (KAN) pup2::pup2-T82C-6HA (HYG)*	S2
TG681	MATα *rpt2::rpt2-L437C (KAN) pre6::pre6- C32A C46A N79C-6HA (HYG)*	S2
TG629	MATα *rpt3::rpt3-K428C (KAN) pre8::pre8-G79C-6HA (HYG)*	S2
TG536	MATα *rpt4::rpt4-L437C (NAT) scl1::scl1-I87C-6HA (HYG)*	S2
TG562	MATα *rpt5::rpt5-A434C (NAT) pre10::pre10-I82C-6HA (HYG)*	S2
TG568	MATα *rpt6::rpt6-K405C (NAT) pre9::pre9-T81C-6HA (HYG)*	S2

*All strains listed in part A have a background genotype of sDL66 (ref. 8): *lys2-801 leu2-3, 2-112 ura3-52 his3-Δ200 trp1-1 rpn11::RPN11-TEVProA(HIS3).* All Rpt salt-bridge and α subunit mutants were initially constructed in strain sDL66. Rpt C-terminal Cys mutants were made by transformation of strain DF5 (ref. 9) and subsequent dissection of the diploids. Double mutants were constructed by mating and tetrad analysis. Note α1 is encoded by *SCL1*, α2 by *PRE8*, α3 by *PRE9*, α4 by *PRE6*, α5 by *PUP2*, α6 by *PRE5*, and α7 by *PRE10.*

**All strains listed in part B have a background genotype of SUB61 (ref. 9):*lys2-801 leu2-3, 2-112 ura3-52 his3-Δ200 trp1-1).*

Supplementary table 2. Yeast strains used to screen for Rpt-α pair crosslinking

	Rpt1-N467C	**Rpt2-L437C**	**Rpt3-K428C**	**Rpt4-L437C**	**Rpt5-A434C**	**Rpt6-K405C**	**Figure**
α1-I87C	TG522	TG612	TG627	TG536	TG550	TG564	2
α2-G79C	TG524	TG615	TG629	TG538	TG552	TG566	S5
α3-T81C	TG526	TG617	TG630	TG540	TG554	TG568	4
α4-N79C	TG528	TG619	TG633	TG542	TG556	TG570	3
α4-W.T.	TG1021	TG1023	TG1025	TG1027	TG1029	TG1031	3
α5-T82C	TG530	TG621	TG635	TG544	TG558	TG572	2
α6-A78C	TG532	TG623	TG637	TG546	TG560	TG574	S5
α6-A78C a5-C117A	TG973	TG975	TG977	TG979	TG981	TG983	5
α7-I82C	TG534	TG625	TG639	TG548	TG562	TG576	S5
α7-I82C a6-C113A	TG777	TG779	TG781	TG783	TG1137	TG787	5

All strains in this table are α mating type and have the background genotype of SUB61 (ref. 9) : *lys2-801 leu2-3, 2-112 ura3-52 his3-Δ200 trp1-1.* The marker for each mutated gene is as listed in table S1 part A.

Supplemental references

1. **Park, S. et al. Hexameric assembly of the proteasomal ATPases is templated through their C termini. *Nature* 459, 866-70 (2009).**
2. **Groll, M. et al. Structure of 20S proteasome from yeast at 2.4 A resolution. *Nature* 386, 463-71 (1997).**
3. **Zhang, F. et al. Structural insights into the regulatory particle of the proteasome from Methanocaldococcus jannaschii. *Molecular cell* 34, 473-84 (2009).**
4. **Djuranovic, S. et al. Structure and activity of the N-terminal substrate recognition domains in proteasomal ATPases. *Molecular cell* 34, 580-90 (2009).**
5. **Saeki, Y., Toh, E.A., Kudo, T., Kawamura, H. & Tanaka, K. Multiple proteasome-interacting proteins assist the assembly of the yeast 19S regulatory particle. *Cell* 137, 900-13 (2009).**
6. **Kaneko, T. et al. Assembly pathway of the Mammalian proteasome base subcomplex is mediated by multiple specific chaperones. *Cell* 137, 914-25 (2009).**
7. **Funakoshi, M., Tomko, R.J., Jr., Kobayashi, H. & Hochstrasser, M. Multiple assembly chaperones govern biogenesis of the proteasome regulatory particle base. *Cell* 137, 887-99 (2009).**
8. **Leggett, D.S. et al. Multiple associated proteins regulate proteasome structure and function. *Molecular cell* 10, 495-507 (2002).**
9. **Finley, D., Ozkaynak, E. & Varshavsky, A. The yeast polyubiquitin gene is essential for resistance to high temperatures, starvation, and other stresses. *Cell* 48, 1035-46 (1987).**